

Novel Luminescent Hexanuclear Platinum(II) Alkynyl Complex: Molecular Lego from a Face-to-Face Dinuclear Platinum(II) Building Block

Chi-Kuen Hui, Ben Wai-Kin Chu, Nianyong Zhu, and Vivian Wing-Wah Yam*

Center for Carbon-Rich Molecular and Nano-scale Metal-based Materials Research, Department of Chemistry, and Open Laboratory of Chemical Biology of the Institute of Molecular Technology for Drug Discovery and Synthesis, The University of Hong Kong, Pokfulam Road, Hong Kong, P.R. China

Received April 30, 2002

A novel luminescent hexanuclear platinum(II) complex, $[\text{Pt}_2(\mu\text{-dppm})_2(\text{C}\equiv\text{CC}_5\text{H}_4\text{N})_4\{\text{Pt}(\text{trpy})\}_4](\text{CF}_3\text{SO}_3)_8$ (trpy = 2,2':6',2''-terpyridine), was successfully synthesized by using the face-to-face dinuclear platinum(II) ethynylpyridine complex $[\text{Pt}_2(\mu\text{-dppm})_2(\text{C}\equiv\text{CC}_5\text{H}_4\text{N})_4]$ as the building block.

Over the past decade, the formation of discrete supramolecular entities driven and held together through metal coordination has remained an intense area of study.^{1,2} Nanoscale supramolecular arrays that possess unique mechanical, chemical, or optical properties were assembled with rigid inorganic and organometallic host species based on transition metal corners and difunctional organic ligand bridges.^{2,3} Dinuclear d^8-d^8 metal complexes, with well defined metal–metal distances, are well-known to exhibit interesting spectroscopic and luminescence behavior, which have been extensively studied, in part because of the interesting observation of weak metal–metal interactions.⁴ Despite the rigidity of the framework and their interesting

spectroscopic properties, no reports were made on the use of face-to-face dinuclear d^8 metal complexes as the building block for supramolecular assemblies. Recently, we synthesized a number of dinuclear platinum(II) alkynyl complexes and studied their luminescence properties.^{5,6} It is believed that the face-to-face dinuclear platinum(II) alkynyl core could be utilized as versatile building blocks for the construction of high-nuclearity supramolecular platinum(II) complexes. Herein are described the synthesis and structural characterization of a face-to-face dinuclear platinum(II) alkynyl complex with ethynylpyridine groups, $[\text{Pt}_2(\mu\text{-dppm})_2(\text{C}\equiv\text{CC}_5\text{H}_4\text{N})_4]$ (**1**), and the first report on the assembly, characterization, and X-ray crystal structure of a face-to-face hexanuclear platinum(II) ethynylpyridine complex, $\{\text{Pt}_2(\mu\text{-dppm})_2(\text{C}\equiv\text{CC}_5\text{H}_4\text{N})_4[\text{Pt}(\text{trpy})]_4\}(\text{CF}_3\text{SO}_3)_8$ (**2**) (Scheme 1).

Complex **1** was synthesized according to modification of a literature procedure for $[\text{Pt}_2(\mu\text{-dppm})_2(\text{C}\equiv\text{CPh})_4]$.⁷ Reaction of **1** with 4 equiv of $[\text{Pt}(\text{trpy})(\text{MeCN})](\text{OTf})_2$ ⁸ in methanol under an inert atmosphere of nitrogen gave a bright yellow precipitate. Recrystallization from acetonitrile–diethyl ether afforded **2** as air-stable orange-yellow crystals in 85% yield. The identities of **1** and **2** were confirmed by satisfactory elemental analyses, positive FAB- and ESI-MS, and ¹H and ³¹P NMR spectroscopy. The solid-state structures were established by X-ray crystallography.⁹

Figure 1 shows the perspective drawing of **1**. It shows a face-to-face arrangement with two mutually eclipsed platinum atoms bridged by two dppm ligands to form an eight-

* To whom correspondence should be addressed. E-mail: wwyam@hku.hk.

- (1) (a) Baxter, P.; Lehn, J. M.; DeCian, A. *Angew. Chem., Int. Ed. Engl.* **1993**, *32*, 69. (b) Amabilino, D. B.; Stoddart, J. F. *Chem. Rev.* **1995**, *95*, 2725. (c) Lehn, J. M. *Supramolecular Chemistry*; VCH Publisher: New York, 1995.
- (2) (a) Fujita, M.; Umamoto, K.; Yoshizawa, M.; Fujita, N.; Kusakawa, T.; Biradha, K. *Chem. Commun.* **2001**, 509. (b) Leininger, S.; Olenyuk, B.; Stang, P. J. *Chem. Rev.* **2000**, *100*, 853. (c) Caulder, D. L.; Raymond, K. N. *Acc. Chem. Res.* **1999**, *32*, 975.
- (3) (a) Fujita, M.; Kwon, Y. J.; Washizu, S.; Ogura, K. *J. Am. Chem. Soc.* **1994**, *116*, 1151. (b) Beer, P. D.; Szemes, F.; Balzani, V.; Sala, C. M.; Drew, M. G. B.; Dent, S. W.; Maestri, M. *J. Am. Chem. Soc.* **1997**, *119*, 11864. (c) Belanger, S.; Hupp, J. T. *Angew. Chem., Int. Ed.* **1999**, *38*, 2222.
- (4) (a) Roundhill, D. M.; Gray, H. B.; Che, C. M. *Acc. Chem. Res.* **1989**, *22*, 55. (b) Balch, A. L. *J. Am. Chem. Soc.* **1976**, *98*, 8049. (c) Inga, M.; Kenney, S.; Kenney, J. W.; Crosby, G. A. *Organometallics* **1986**, *5*, 230. (d) Che, C. M.; Yam, V. W. W.; Wong, W. T.; Lai, T. F. *Inorg. Chem.* **1989**, *28*, 2908. (e) Smith, D. C.; Gray, H. B. *Coord. Chem. Rev.* **1990**, *100*, 169. (f) Yip, H. K.; Che, C. M.; Zhou, Z. Y.; Mak, T. C. W. *J. Chem. Soc., Chem. Commun.* **1992**, 1369. (g) Striplin, D. R.; Crosby, G. A. *J. Phys. Chem.* **1995**, *99*, 7977. (h) Lewis, N. S.; Mann, K. R.; Gordon, J. G., II; Gray, H. B. *J. Am. Chem. Soc.* **1976**, *98*, 7461. (i) Yip, H. K.; Lin, H. M.; Wang, Y.; Che, C. M. *J. Chem. Soc., Dalton Trans.* **1993**, 2939.

- (5) (a) Wong, K. M. C.; Hui, C. K.; Yu, K. L.; Yam, V. W. W. *Coord. Chem. Rev.* **2002**, *229*, 123. (b) Yam, V. W. W.; Yu, K. L.; Wong, K. M. C.; Cheung, K. K. *Organometallics* **2001**, *20*, 721. (c) Yam, V. W. W.; Hui, C. K.; Wong, K. M. C.; Zhu, N.; Cheung, K. K. *Organometallics* **2002**, *21*, 4326.
- (6) (a) Yam, V. W. W. *J. Photochem. and Photobiol., A* **1997**, *106*, 75. (b) Yam, V. W. W.; Lo, K. K. W.; Fung, W. K. M.; Wang, C. R. *Coord. Chem. Rev.* **1998**, *171*, 17. (c) Yam, V. W. W.; Lo, K. K. W. *Chem. Soc. Rev.* **1999**, *28*, 323. (d) Yam, V. W. W.; Lo, K. K. W.; Wong, K. M. C. *J. Organomet. Chem.* **1999**, *578*, 3.
- (7) Pringle, P. G.; Shaw, B. L. *Chem. Commun.* **1982**, 581.
- (8) Yam, V. W. W.; Tang, R. P. L.; Wong, K. M. C.; Cheung, K. K. *Organometallics* **2001**, *20*, 4476.

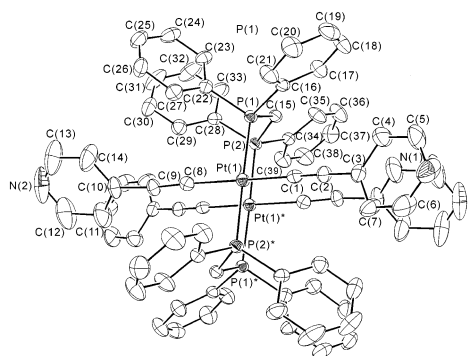
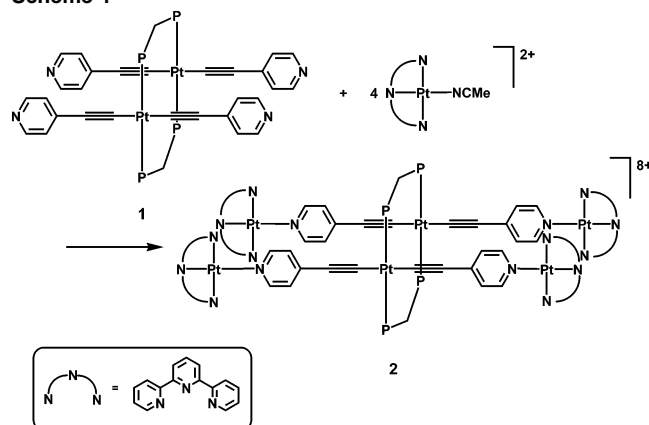


Figure 1. Perspective view of $[\text{Pt}_2(\mu\text{-dppm})_2(\text{C}\equiv\text{CC}_5\text{H}_4\text{N})_4]$ (**1**). The H atoms have been omitted for clarity. Thermal ellipsoids are shown at 30% probability level.

Scheme 1



membered ring. Each platinum atom exhibits a distorted square planar geometry with the two alkyne groups $[\text{C}-\text{Pt}-\text{C}, 169.3(3)^\circ]$ and the two bridging dppm phosphorus atoms $[\text{P}-\text{Pt}-\text{P}, 176.4(1)^\circ]$ arranged in a *trans*-disposition. The short intramolecular $\text{Pt}(1)-\text{Pt}(1)^*$ distance of $3.285(1) \text{ \AA}$, which is comparable to that of the related $[\text{Pt}_2(\mu\text{-dppm})_2(\text{CN})_4]$ (3.30 \AA) and is somewhat longer than that of $[\text{Pt}_2(\text{pop})_4]^{4-}$ (2.95 \AA), indicates the presence of a weak $\text{Pt}\cdots\text{Pt}$ interaction.⁴

Figure 2 shows the perspective drawing of the complex cation of **2**. The terpyridyl $\text{Pt}(\text{II})$ shows a distorted square planar geometry, as is required by the bite angle exerted by the terpyridine ligand. The dihedral angle between the plane of the pyridine ring and that of $\text{Pt}(\text{trpy})$ is ca. 66.51° . Similar dihedral angles and near-orthogonal orientation of the pyridine ring with respect to the platinum square plane have also been observed in the related pyridine-containing $\text{Pt}(\text{C}^{\wedge}\text{N}^{\wedge}\text{C})$ and $\text{Pt}(\text{C}^{\wedge}\text{N}^{\wedge}\text{N})$ complexes.¹⁰ In complex **2**, a comparatively stronger $\text{Pt}\cdots\text{Pt}$ interaction between the two platinum atoms in the $\text{Pt}_2(\text{dppm})_2$ core than that in **1** was

observed, as reflected from the shorter $\text{Pt}\cdots\text{Pt}$ distance [**2**, $3.178(1) \text{ \AA}$ vs **1**, $3.285(1) \text{ \AA}$]. The contraction of the $\text{Pt}\cdots\text{Pt}$ distance within the $\text{Pt}_2(\text{dppm})_2$ core in **2** compared to **1** is thought to originate predominantly from electronic effects rather than from steric grounds. The reduced electron density on the dinuclear platinum centers in **1** would probably favor metal–metal interactions to occur in order to compensate for the loss of electron density upon coordination of the $\text{Pt}(\text{trpy})$ units. In general, steric effects are also known to affect the metal–metal separation, in which an increased bulk of the alkyne ligands would cause the bending of the $\text{C}-\text{Pt}-\text{C}$ bond, forcing the two Pt centers to approach each other more closely.^{5c} The metal–metal interaction has also been correlated to the steric demand of the coordinated ligands as reflected by the pyramidity effect.¹¹ However, on the basis of steric arguments alone, the smaller observed deviation of the $\text{C}-\text{Pt}-\text{C}$ angle from 180° in **2** [$6.0(7)^\circ$] compared to **1** [$10.7(3)^\circ$] is not in agreement with the shorter $\text{Pt}\cdots\text{Pt}$ distance observed in **2** [$\text{Pt}\cdots\text{Pt}$, $3.178(1) \text{ \AA}$] compared to **1** [$\text{Pt}\cdots\text{Pt}$, $3.285(1) \text{ \AA}$]. Therefore, it is likely that the electronic effect plays a more dominant role in governing the metal–metal distance in the present system.

The two adjacent peripheral $\text{Pt}(\text{trpy})$ moieties are in parallel orientation, with an interplanar distance of ca. 3.67 \AA , suggesting the presence of some π -stacking interactions between the two terpyridyl units.¹² However, the $\text{Pt}(\text{trpy})$ planes are slanted at an angle of ca. 34.66° to the $\text{P}-\text{Pt}-\text{P}$ axis, giving a $\text{Pt}\cdots\text{Pt}$ distance of $5.079(1) \text{ \AA}$, suggestive of no $\text{Pt}\cdots\text{Pt}$ interactions between the peripheral platinum atoms.

The electronic absorption spectrum of **1** in ethanol–dichloromethane (1:4 v/v) shows a low-energy absorption band at ca. 368 nm , with low-energy tails extending to ca. 450 nm . With reference to previous spectroscopic work on the related face-to-face dinuclear platinum(II) alkyne complexes,⁵ the low-energy absorption band at 368 nm is assigned as a spin-allowed metal–metal-to–ligand charge transfer (MMLCT) [$d_\sigma^*(\text{Pt}_2) \rightarrow p_\sigma(\text{Pt}_2)/\pi^*(\text{C}\equiv\text{CR})$] transition, while the low-energy tails are assigned as spin-forbidden MMLCT transitions. The electronic absorption spectrum of **2** in acetone shows a low-energy absorption band at ca. 416 nm . It is suggested that the low-energy absorption band may involve a $d\pi(\text{Pt}) \rightarrow \pi^*(\text{trpy})$ metal-to–ligand charge transfer (MLCT) transition because similar absorption bands attributed to MLCT transition are observed in other related platinum(II) terpyridyl systems.¹³

Upon excitation at $\lambda > 350 \text{ nm}$, **1** exhibits strong luminescence in the solid state and in solutions both at room

(9) Crystal data for **1**: $\text{C}_{82}\text{H}_{70}\text{N}_4\text{O}_2\text{P}_4\text{Pt}_2$; $M_r = 1657.48$, triclinic, space group $P1$, $a = 10.648(2) \text{ \AA}$, $b = 12.848(3) \text{ \AA}$, $c = 14.174(3) \text{ \AA}$, $\alpha = 66.82(2)^\circ$, $\beta = 87.78(2)^\circ$, $\gamma = 87.09(3)^\circ$, $V = 1779.9(7) \text{ \AA}^3$, $T = 293 \text{ K}$, $Z = 1$, $D_c = 1.546 \text{ g cm}^{-3}$, $\mu(\text{Mo K}\alpha) = 4.066 \text{ mm}^{-1}$, 10398 reflections measured, 5602 unique ($R_{\text{int}} = 0.0394$) which were used in all calculations. The final $R(F^2)$ was 0.0361 [$I > 2\sigma(I)$]. Crystal data for **2**: $\text{C}_{150}\text{H}_{114}\text{F}_{24}\text{N}_{18}\text{O}_{26}\text{P}_4\text{Pt}_6\text{S}_8$; $M_r = 4591.49$, monoclinic, space group $P2_1/c$, $a = 14.013(3) \text{ \AA}$, $b = 14.377(3) \text{ \AA}$, $c = 46.275(9) \text{ \AA}$, $\beta = 97.12(3)^\circ$, $V = 9251(3) \text{ \AA}^3$, $T = 253 \text{ K}$, $Z = 2$, $D_c = 1.648 \text{ g cm}^{-3}$, $\mu(\text{Mo K}\alpha) = 4.733 \text{ mm}^{-1}$, 31324 reflections measured, 11726 unique ($R_{\text{int}} = 0.0615$) which were used in all calculations. The final $R(F^2)$ was 0.0558 [$I > 2\sigma(I)$].

(10) (a) Lu, W.; Chan, M. C. W.; Cheung, K. K.; Che, C. M. *Organometallics* **2001**, *20*, 2477. (b) Yip, J. H. K.; Suwarno; Vittal, J. J. *Inorg. Chem.* **2000**, *39*, 3537. (c) Chernega, A.; Droz, A. S.; Prout, K.; Vilaivan, T.; Weaver, G. W.; Lowe, G. J. *Chem. Research* **1996**, 402. (11) Aullón, G.; Alemany, P.; Alvarez, S. *Inorg. Chem.* **1996**, *35*, 5061. (12) (a) Büchner, R.; Cunningham, C. T.; Field, J. S.; Haines, R. J.; McMillin, D. R.; Summerton, G. C. *J. Chem. Soc., Dalton Trans.* **1999**, 711. (b) Bailey, J. A.; Hill, M. G.; Marsh, R. E.; Miskowski, V. M.; Schaefer, W. P.; Gray, H. B. *Inorg. Chem.* **1995**, *34*, 4591. (c) Hunter, C. A.; Sanders, J. K. M. *J. Am. Chem. Soc.* **1990**, *112*, 5525. (13) (a) Aldridge, T. K.; Stacy, E. M.; McMillin, D. R. *Inorg. Chem.* **1994**, *33*, 722. (b) Bailey, J. A.; Miskowski, V. M.; Gray, H. B. *Inorg. Chem.* **1993**, *32*, 369. (b) Yip, H. K.; Cheng, L. K.; Cheung, K. K.; Che, C. M. *J. Chem. Soc., Dalton Trans.* **1993**, 2933.

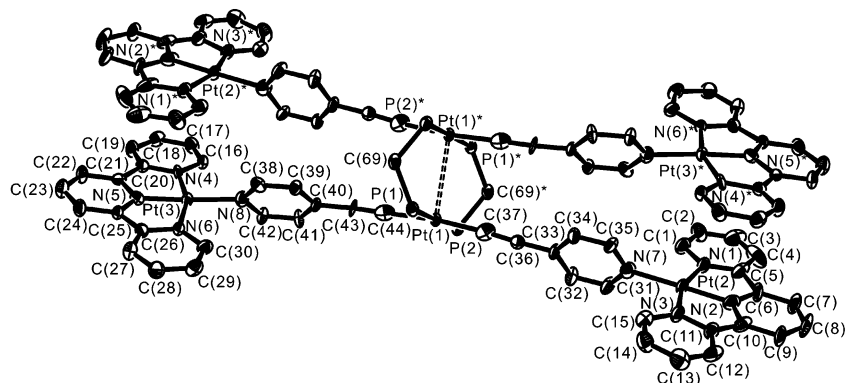


Figure 2. Perspective view of the complex cation of $[\text{Pt}_2(\mu\text{-dppm})_2(\text{C}\equiv\text{CC}_5\text{H}_4\text{N})_4\{\text{Pt}(\text{trpy})\}_4](\text{CF}_3\text{SO}_3)_8$ (**2**). The H atoms and C atoms of phenyl rings of dppm have been omitted for clarity. Thermal ellipsoids are shown at 20% probability level.

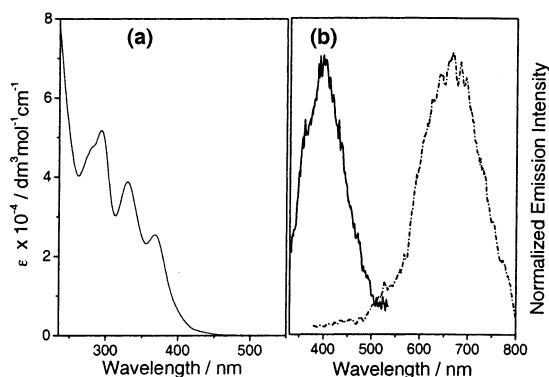


Figure 3. (a) UV-vis absorption spectrum of $[\text{Pt}_2(\mu\text{-dppm})_2(\text{C}\equiv\text{CC}_5\text{H}_4\text{N})_4]$ (**1**). (b) Excitation (—) and emission (---) spectra of **1** in EtOH- CH_2Cl_2 (1:4 v/v) at 298 K. Excitation wavelength at 355 nm.

temperature and at 77 K. Two emission bands at 515 and 635 nm are observed in the steady-state emission spectrum of **1** in EtOH- CH_2Cl_2 (1:4 v/v) at 77 K. The two emission bands are found to have different lifetimes, both in micro-second range, probably arising from different origins.¹⁴ With reference to previous spectroscopic work,^{5b} the higher energy emission band observed at ca. 515 nm is tentatively assigned as intraligand phosphorescence of the bridging diphosphine ligands. The emission spectrum of **1** in the solid state at 77 K shows an emission band at ca. 605 nm, while at room temperature in ethanol-dichloromethane (1:4 v/v) an emission band at ca. 670 nm is observed; both of these are ascribed to phosphorescence derived from the ³MMLCT state. Figure 3 shows the excitation and time-resolved emission spectra of **1** in EtOH- CH_2Cl_2 (1:4 v/v) at 298 K. The close resemblance of the excitation band to the low-energy tail at ca. 400–450 nm in the electronic absorption spectrum is supportive of a ³MMLCT origin.

Complex **2** exhibits strong luminescence at ca. 520 nm at 77 K in ethanol-methanol (4:1 v/v) glass, which may probably arise from metal-perturbed ligand-centered phosphorescence. The solid state of **2** in 77 K exhibits strong luminescence at ca. 620 nm which is also ascribed to

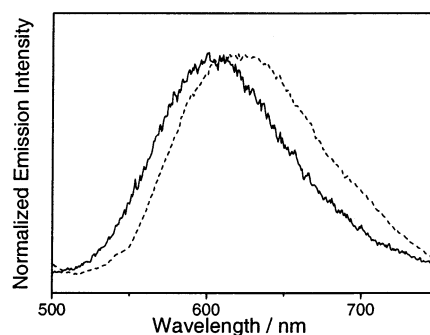


Figure 4. Normalized emission spectra of $[\text{Pt}_2(\mu\text{-dppm})_2(\text{C}\equiv\text{CC}_5\text{H}_4\text{N})_4]$ (**1**) (—) and $[\text{Pt}_2(\mu\text{-dppm})_2\{\text{C}\equiv\text{CC}_5\text{H}_4\text{NPt}(\text{trpy})\}_4](\text{CF}_3\text{SO}_3)_8$ (**2**) (---) in the solid state at 77 K. Excitation wavelength at 355 nm for **1** and at 400 nm for **2**.

phosphorescence derived from the ³MMLCT state. The red-shift of the emission band of **2** relative to that of **1** (Figure 4) is probably attributed to the increased Pt···Pt interaction due to a shrinkage of the Pt···Pt bond distance in the $\text{Pt}_2(\text{dppm})_2$ core in the hexanuclear structure as well as an increase in the π -accepting ability of the ethynylpyridine units upon coordination of the Pt(trpy) moieties.

The present work demonstrates a facile and high-yield synthesis of a high-nuclearity supramolecular platinum complex using a face-to-face dinuclear platinum complex as the building block. The application of this class of compounds in transition-metal-mediated supramolecular self-assembly shows great potential and is now in progress.

Acknowledgment. V. W.-W. Y. acknowledges support from The University of Hong Kong Foundation for Educational Development and Research Limited and the University Grants Committee Area of Excellence Scheme. The work described in this paper has been supported by the Research Grants Council of the Hong Kong Special Administrative Region, China (Project HKU7123/00P). C.-K. H. acknowledges the receipt of a postgraduate studentship, and N. Z., the receipt of a university postdoctoral fellowship, both administered by The University of Hong Kong, and B. W.-K. C. the receipt of a postdoctoral fellowship supported by the Generic Drug Research Program of The University of Hong Kong.

Supporting Information Available: Characterization, crystallographic data, and photophysical data of **1** and **2**. This material is available free of charge via the Internet at <http://pubs.acs.org>. IC025685D

(14) The attribution of the high energy emission of **1** to be due to the presence of a small amount of impurity in less than 1%, most likely the mononuclear *trans*- $[\text{Pt}(\text{dppm})_2(\text{C}\equiv\text{CC}_5\text{H}_4\text{N})_2]$ complex, is not favored, because the emission energy of the related *trans*- $[\text{Pt}(\text{dppm})_2(\text{C}\equiv\text{CC}_6\text{H}_5)_2]$ is known to occur at higher energy (see ref 4i). Although the possibility of the presence of an impurity cannot be completely eliminated, we do not favor this assignment.